frontiers | Frontiers in Environmental Science

TYPE Original Research
PUBLISHED 29 December 2025
DOI 10.3389/fenvs.2025.1734892

OPEN ACCESS

EDITED BY
Jun Zhou,
Chinese Academy of Sciences (CAS), China

REVIEWED BY
Tianzhi Huang,
Mianyang Normal University, China
Shihai Cui,
Nanjing Normal University, China
Huimin Feng,
Nanjing Agricultural University, China

*CORRESPONDENCE
Buyun Du,
duby@jsou.edu.cn
Ting Sun,
tsun64@uwo.ca

RECEIVED 29 October 2025
REVISED 21 November 2025
ACCEPTED 26 November 2025
PUBLISHED 29 December 2025

CITATION
Huang Z, Du B, Sun T and Ji D (2025) Biochar mitigates soil–rice accumulation of highly bioavailable heavy metals from atmospheric deposition.
Front. Environ. Sci. 13:1734892.
doi: 10.3389/fenvs.2025.1734892

Biochar mitigates soil–rice accumulation of highly bioavailable heavy metals from atmospheric deposition

Zhaoqin Huang[1], Buyun Du[1]*, Ting Sun[2]* and Dongliang Ji[1]

[1]College of Environmental Ecology, Jiangsu Open University, Nanjing, China, [2]School of Environmental Science and Engineering, Shandong University, Qingdao, China

Little is known regarding the uptake of heavy metal(loid)s (HMs) by crops from atmospheric deposition. In this study, we examined the uptake and transport of HMs (copper, zinc, arsenic, cadmium, and lead) in rice plants through both root and foliar pathways, and the reduction of HMs in rice resulting from soil biochar applications. Our findings indicate that HMs from dust and rainfall were more mobile and bioavailable than those from slag, significantly affecting the soluble and exchangeable fractions of HMs in the soil, soil solution, and fractions detected by the diffusive gradients in thin films (DGT) technique. Rice plants exhibited a preference for absorbing atmospherically deposited HMs through both foliar and root pathways; however, the efficiency of HM uptake and translocation rates via direct foliar uptake was lower than that of root uptake from the soil. The application of biochar was found to decrease HM (Cu, Zn, Pb, and Cd) concentrations in soil mobile fractions, soil solutions, and DGT extractions, with the exception of As; this demonstrates an effective method to mitigate HM accumulation in rice. This study highlights the high risk of crop contamination in areas with high atmospheric HM loads and suggests that reducing atmospheric HM deposition and implementing soil remediation can mitigate ecological risks.

KEYWORDS

simulation experiment, biochar application, rice accumulation, node, thin films technique

1 Introduction

With an increasing demand for metal resources driven by rapid economic growth worldwide, large amounts of heavy metal(loid)s (HMs) have been released in mining and smelting processes (Du et al., 2023). The global emission inventory of copper (Cu), zinc (Zn), cadmium (Cd), lead (Pb), and arsenic (As) from anthropogenic atmospheric emissions were up to 46,328, 43,840, 2,246, 47,669, and 8,460 tons per year, respectively (Zhu et al., 2020). Nonferrous metals smelting is considered as the largest human sources of atmospheric As and Cd (51%–71%) and an important contributor of atmospheric Cu, Zn, and Pb (26%–35%). These HM-laden particles, transported through the atmosphere, ultimately settle on the earth's surface and contribute to the legacy of soil contamination by historical emissions, posing considerable ecological risks (Ji et al., 2023; Zhou et al., 2024a).

HM emission and deposition has decreased in Europe and North America over both short and long timeframes (McLaughlin et al., 2021), but atmospheric deposition is still a

critical pollution source in agricultural ecosystems far from point sources, especially in Asia (Peng et al., 2019). Metal mining and smelting, in particular, generate emissions of atmospheric particles with high HM concentrations (Zhu et al., 2020), leading to extremely high atmospheric HM inputs in nearby agricultural soils, exceeding other sources by orders of magnitude (Mi et al., 2023). In soils, newly deposited HMs have been found to be bound preferentially to the soil aggregate surface, while residual HMs fraction showed a higher percentage in aggregate cores (Wilcke and Kaupenjohann, 1998; Shahid et al., 2020) and mainly presented in soil solutions as bioavailable fractions (Zhou et al., 2024b). HMs from recent atmospheric deposition are thus highly available to plants via root uptake (Luo et al., 2019; Yan et al., 2022), yet we lack direct observations of plant bioaccumulation and the uptake of newly deposited HMs compared to other input sources of HMs in soils. In addition, atmospherically deposited HMs can potentially be directly absorbed by foliage, but the mechanism is still poorly understood (Shahid et al., 2017; Yan et al., 2022), especially for foliar uptake and translocation in cereal crops. Foliage can take up the HMs bonding in atmospheric particulates via stomata, aqueous pores, cracks, and lenticel, primarily through the ectodesmata in the cuticular membrane or epidermal cell wall via active transport in the subjacent cell symplastic pathway (Shahid et al., 2021; Shoaib and Javaid, 2021).

Recent studies suggest that HMs from atmospheric deposition during the rice growing seasons were significantly absorbed by rice plants, accounting for 6%–77% of the Cd, Cu, Zn, and Pb in grains (Feng et al., 2019; Xia et al., 2024; Xia et al., 2023; Zhou J. et al., 2020). Studies have investigated the immobilization of HMs in soils to reduce their accumulation in rice (Li et al., 2022; Liu Q. et al., 2024), but only one has investigated whether lime amendment can reduce newly deposited HM mobilization in soils (Cui et al., 2024). This found that lime applications significantly decrease the HMs in soil solution when exposed to atmospheric deposition. However, no studies have investigated whether soil amendments can reduce deposited HM accumulation in rice plants. Biochar is a carbon-rich organic material derived from the pyrolysis process of various organic sources such as wood waste, sludge, municipal solid waste, crop straw, and other organic matter (Chen et al., 2024; Oral et al., 2024). Numerous studies have highlighted the potential benefits of biochar in terms of carbon sequestration, enhancement of soil fertility, and the recycling of agricultural waste (Oral et al., 2024; Yang et al., 2024). Recent investigations have also confirmed the efficacy of biochar in HM immobilization in soils. Chen et al. (2024) conducted a hierarchical meta-analysis based on 276 published studies, finding that all types of biochar significantly decrease available HM concentrations in soil and their accumulation in crop tissues. Biochar amendments can influence microbial reduction in soils by supplying carbon (organic) and nutrients, controlling it to a lower Eh and higher pH in the soil (Islam et al., 2023); meanwhile, the suite of unique chemical and physical properties of biochar, including a highly specific surface area, a well-developed porous structure, abundant functional groups, and a strong negative charge, are instrumental in reducing the bioavailability of HMs in soil–crop systems (Li et al., 2022; Sachdeva et al., 2023; Islam et al., 2023).

We used factorial design to test the effects of both modes of HM deposition and uptake as well as soil amendments on HM uptake by rice. The study utilized a simulation experiment conducted in a greenhouse and employed various analytical methods such as sequential extraction, soil solution, and diffusive gradients in thin films (DGT) technique. The hypothesis posited was that HMs deposited from the atmosphere are more readily bioavailable for assimilation than other sources like slag and that biochar applications can effectively reduce the accumulation of HMs in rice plants.

2 Experimental procedures

2.1 Greenhouse experiment design

The soils were collected in Jiangxi Province, with properties shown in Supplementary Table S1. Simulation experiments were conducted by soil additions of 1 g and 2.5 g of dust to simulate dry deposition, pot irrigation of 30 L and 75 L rainwater to simulate wet deposition, 100 g and 250 g slag to represent another source of the local environment of a Cu smelter, and foliar application of 1 g and 2.5 g of dust to simulate foliar uptake of dry deposition (Table 1). The dust and rainfall were collected 1 km from the smelter 1 month before our experiment. The amount of dust and rainwater added is approximately equivalent to 5 years of Cd deposition fluxes near the smelter (Zhou et al., 2024b) where the soil was collected, so as to more effectively and directly reflect the enrichment effect of the atmospheric precipitation of heavy metals in the soil–rice system and the application effect of biochar amendments. Slag was collected from smelting residue of ore and was used to compare Cd bioavailability with the source from atmospheric deposition. Dust was sampled from pulse-pack dust catchers deployed in the Cu smelter. The dust was used to simulate dry deposition, which had a similar major mineralogical composition with the dry deposition sample (Liu et al., 2019; Liu et al., 2021) and higher mobile fractions (Supplementary Table S2). For all soil application treatments, additional 25 g biochar applications were performed to investigate if they could reduce the soil bioavailability of HMs and plant accumulation. Each plastic pot (height 20 cm, top and bottom diameter of 25 cm and 22 cm respectively) was filled with 5 kg of soil on a dry-weight basis. Biochar was added at doses of 0.5% w/w in the soil (Shen et al., 2016), thoroughly mixed, and then incubated for 2 weeks under flooding conditions. The biochar was produced from rice husk under 550 °C (Zhejiang Yangtze River Delta Junong Technology Development Co., Ltd.). Dust and slag were added separately and mixed in pots of 5 kg background soil. Rainwater collected from a site with high deposition levels was utilized to mimic wet deposition and provide irrigation during the rice cultivation period. Two deposition dosages (low (L) and high (H)) were used and represented approximately 10- and 5-year dry Cd deposition loads. There were in total 15 treatments with experimental triplicates, including a control (CK), soil with slag (H-S and L-S) and slag and biochar (H-SB and L-SB), soil with dust (H-D and L-D) and dust and biochar (H-DB and L-DB), soil irrigated with rainfall (H-R and L-R) and rainfall and biochar (H-RB and L-RB), and foliar dust application (H-F and L-F) (Table 1). The placement of replicate pots adopted a randomization design to avoid differences in light and temperature in different areas.

TABLE 1 Pot experimental design in this study.

Treatment	Addition of simulated experiment
CK	Background soil
L-S	100 g slag per pot mixed with soil
L-SB	100 g slag and 25 g biochar per pot mixed with soil
H-S	250 g slag per pot mixed with soil
H-SB	250 g slag and 25 g biochar per pot mixed with soil
L-D	1 g dust per pot mixed with soil
L-DB	1 g dust and 25 g biochar per pot mixed with soil
H-D	2.5 g dust per pot mixed with soil
H-DB	2.5 g dust and 25 g biochar per pot mixed with soil
L-R	1 L water of wet deposition irrigated each time
L-RB	25 g biochar mixed with soil and 1 L water of wet deposition irrigated each time
H-R	2 L water of wet deposition irrigated each time
H-RB	25 g biochar mixed with soil and 2 L water of wet deposition irrigated each time
L-F	1 g dust per pot deposited on adaxial faces of each leaf
H-F	2.5 g dust per pot deposited on adaxial faces of each leaf

The "Wuyouhuazhan" rice variety was used in this study, which is widely cultivated in Jiangxi Province, China. The foliar dust application involved using an applicator brush to apply dust to the upper leaf surfaces during the fully developed leaf stage, following the method described by Xiong et al. (2017), with the same quantities as the soil deposition doses. Each pot contained one seedling for cultivation. The entire growth cycle of rice lasted for 105 days, since the seedlings were transported to the pots. The pots were kept flooded 1 week before harvest.

2.2 Sample collection and analyses

The rice samples were washed in the laboratory with tap water, 1% hydrochloric acid, and deionized water, employing a soft-bristled brush to eliminate surface contaminants. We used 1% hydrochloric acid to avoid adsorption of the HMs in the surface of the rice tissues, while it cannot dissolve the HMs in the rice tissues (Xia et al., 2024). Following this, the whole rice plants were categorized into root, stem, leaf, husk, and brown rice components and stored in paper containers. The rice components were dehydrated at a consistent 60 °C within an oven until reaching a stable weight. The weight of the rice components was then gauged post-drying in the laboratory. Subsequently, the rice tissue samples were thoroughly pulverized into a fine powder using a food crusher, sifted through a 100-mesh sieve, and the processed samples were stored at −20 °C in separate polyethylene bags to prevent any potential contamination. In the case of soil and foliar dust applications, the stems were further segmented into three nodes as the transfer of HMs from root or leaf to rice grain should occur through a couple of nodes in the stem, where HMs are redirected during the process.

During the mature stage, soil profiles were subjected to diffusive gradients in thin films (DGT) measurements on the day prior to rice harvest, with the DGT samples being collected the subsequent day while the soils remained flooded (Fang et al., 2021; Zhou C. et al., 2020). The DGT apparatus consisted of an acrylamide diffusion membrane, synthesized with modified agarose as the cross-linking agent, and with Chelex-100 functioning as the binding membrane for the adsorption of heavy metals (HMs). Additionally, a protective membrane composed of nitrocellulose with a pore size of 0.45 μm was incorporated. DGT technology is recognized as an effective method for identifying the various forms of HMs, thereby enhancing the understanding of their bioavailability and the assessment of their release risks (Gao et al., 2020). This approach provides a more nuanced perspective on the interrelationships among elements compared to traditional methods such as *ex situ* extractions by calcium chloride ($CaCl_2$) and ethylenediamine tetraacetic acid (EDTA) (Ding et al., 2011). The operational procedures for DGT are elaborated in Supplementary Text S1. Additionally, the soil solution was sampled 1 week before rice harvest by an injection syringe connecting to a ceramic lysimeter *in situ* at 10 cm depth, which was buried before rice cultivation. The analysis of HMs in soil and plant samples was conducted through acid digestion, following methodologies established in prior research (Zhou J. et al., 2020). The extraction of HMs from dust, slag, and soil samples was performed using the BCR sequential extraction method, which categorizes the fractions into four groups: F1 (soluble and exchangeable), F2 (reducible), F3 (oxidizable), and F4 (residual), as detailed in Supplementary Text S2. The concentrations of all HMs in the digested and extracted solutions were quantified using inductively coupled plasma mass spectrometry (ICP-MS). Quality control protocols, including blank tests, detection limits, and recovery evaluations utilizing certified reference materials, were implemented and are detailed in Supplementary Table S3. Here, the bioavailable HMs in soils or atmospheric deposition refer to the fraction of HMs that can be taken up by plants, which is shown as HMs measured in soil solutions, DGT, and F1 extractions.

2.3 Data calculation

To calculate the contribution (HM_{DFS}, %) of newly added HM from dust, rainfall, and slag to the rice tissues over the legacy HMs in the control soils, the contribution from soil and foliar exposures was calculated as

$$HM_{DFS} = (HM_{EX} \times M_{EX} - HM_{CK} \times M_{CK}) / (S_{EX} - S_{CK}) \times 100\%, \quad (1)$$

where HM_{DFS} is the HM deposition contribution fraction, HM_{EX} and HM_{CK} represent the HM concentrations in the rice tissues of exposure treatments and control treatment, respectively, M_{EX} and M_{CK} are the tissue masses of exposure treatments and control treatment, respectively, and S_{EX} and S_{CK} are the HM pool in the treatment and control soils for soil applications, while SEX represent the HM mass applied to the leaves in the foliar application treatments.

Except for foliar exposure, the HM bioaccumulation factors (BAFs) were calculated using HM concentrations (mg kg^{-1}) in rice

tissues (HM_t) compared to corresponding soil concentrations (HM_s):

$$BAF = \frac{HM_t}{HM_s}. \quad (2)$$

The average concentrations of HMs in soil fractions and rice tissues were analyzed using a Levene test and two-tailed analysis of variance (ANOVA) conducted with SPSS software (version 16.0, SPSS Inc.). All observed differences in means were deemed statistically significant at the $p = 0.05$ level (two-tailed), with the means presented along with their corresponding standard deviations.

3 Results

3.1 HM fractions in the simulated atmospheric deposition and soils

The total concentrations of Cu, Zn, As, Cd, and Pb were, respectively, 324,000, 77,400, 60,100, 1,910, and 50,600 mg kg^{-1} in the dust, 3,210, 14,800, 590, 20, and 5,440 mg kg^{-1} in the slag, and 2.3, 0.34, 0.88, 0.080, and 3.4 mg L^{-1} in the rainfall. The BCR fractions showed much higher F1 percentages of all the HMs in the dust (15%–78%) than those in the slag samples (6%–38%) (Supplementary Table S2), suggesting that the HMs in the dust, simulating dry deposition, were much more mobile than those in the slag. In the rainfall, more than 85% of the HMs were presented in the dissolved fractions (<0.45 μm).

All the HM concentrations in the exposed treatments were significantly higher than those in the control treatment. The total concentrations of Cu, As, and Cd in the soils were similar between the low and high treatments for both slag and dust addition groups. However, the concentrations of Zn and Pb in the soils were much lower in the dust addition groups than in the slag addition groups. In the rainfall addition treatments, the lowest HM concentrations in the soils were observed, attributed to the lower HM additions (Figure 1). For all HMs, the dominated fractions in the soils are presented in F4, followed by F2, with the lowest observed in F3 and F1 (Supplementary Figure S1). The additions of dust, rainfall, and slag still significantly increased the percentage of bioavailable fraction (F1) (Figure 1; Supplementary Figure S1). Although the concentrations of the mobile and bioavailable fraction in soils subject to rainfall treatments were much lower than those in the slag treatment, the increased percentages were much higher in the rainfall treatments. Additionally, the increased percentages of F1 in the dust treatments were also significantly higher than those in the slag treatments, a result that was consistent with the above-reported Cd fractions in dust, rainfall, and slag.

The accumulation of HMs in crops through root uptake is primarily influenced by the bioavailable HMs present in soil solutions. The application of slag and rainfall significantly enhanced the concentrations of Cu and Cd in the soil solutions (Table 2). Although total soil Cu concentrations in the slag treatments were 1.6–2.2 times higher than those in the rainfall treatments, the Cu concentrations in the solutions were lower in the slag treatments. For the dust treatments, the Cu and Cd concentrations in the soil solutions were much higher than those in the slag treatments, but the soils showed similar total Cu and Cd concentrations. Similar results were observed in the DGT-measured HM concentrations. In the slag and rainfall treatments, similar DGT-measured HM concentrations were observed despite much higher concentrations in the slag treatments. Additionally, Cu, Cd, and As showed similar concentrations in the corresponding low- and high-level treatments of slag and dust, but these concentrations in the DGT-measured treatments were 0.2–3.4 times higher in the dust treatments.

3.2 Biochar application effects on soil HM fractions

Biochar is an amendment that can be extensively utilized in the remediation of HM-contaminated soil across various regions, exhibiting an excellent immobilization effect. In this study, the soil biochar applications also significantly reduced the mobile fractions (F1) to more stable fractions (e.g., F2 and F4). For example, after biochar applications, the F1 fractions of Cu saw reductions of 13%–19%, 31%–32%, and 32%–29% in the slag, dust, and rainfall addition treatments, respectively. Similarly, F2 experienced reductions of 8%–9%, 4%–20%, and 36%–48% under the same conditions. In contrast, the unavailable fractions (F3 + F4) were significantly increased by 18%–86% (Figure 1). Like the Cu fractions, the biochar applications significantly reduced the F1 fractions of Zn by 10%–23%, 4%–16%, and 26%–27%, the F1 fractions of Cd by 10%–25%, 17%–26%, and 77%–87%, and the F1 fractions of Pb by 11%–44%, 29%–46%, and 77%–91% in the slag, dust, and rainfall treatments, respectively. These reductions were accompanied by an increase in the F3 and F4 fractions.

In addition to reducing the mobility of HM in soils, biochar applications have also been found to significantly decrease the HM concentrations in soil solutions (Table 2). Due to instrument detection limits, only the Cu and Cd concentrations in the soil solutions were detectable. The Cu concentrations were significantly reduced by 14%–20%, 17%–20%, and 17%–26%, while the Pb concentrations were reduced by 25%–30%, 24%–31%, and 9%–21% in the slag, dust, and rainfall addition treatments, respectively, following biochar applications. Similar results were observed in DGT-measured HM concentrations, which were also significantly decreased by biochar applications. The DGT-measured concentrations of Cu, Zn, Cd, and Pb were significantly reduced by 13%–38%, 11%–15%, 24%–36%, and 15%–20% in the slag treatments, by 18%–58%, 13%–29%, 33%–34%, 26%–38%, and 28%–32% in the dust treatments, and by 25%–36%, 16%–22%, 58%–62%, 34%–42%, and 21%–26% in the rainfall treatments, respectively, after biochar applications. The reduction percentages were more pronounced in the simulation treatments of atmospheric deposition (dust and slag) than those in the slag treatments because those metals were more mobile and thus more easily mobilized.

Reactions of As differed from Cu, Cd, and Pb in biochar application treatment. The biochar applications did not significantly reduce the F1 fractions of As in all the biochar applications, which was only 3.3%–4.1%, 5.6%–7.8%, and 5.4%–8.3% in the slag, dust, and rainfall addition treatments, respectively. The DGT-measured As in all the biochar applications also did not significantly reduce. The DGT-measured concentrations of As were only reduced by 4.2%–5.1%, 5.3%–8.9%, and 6.2%–7.4% in the slag,

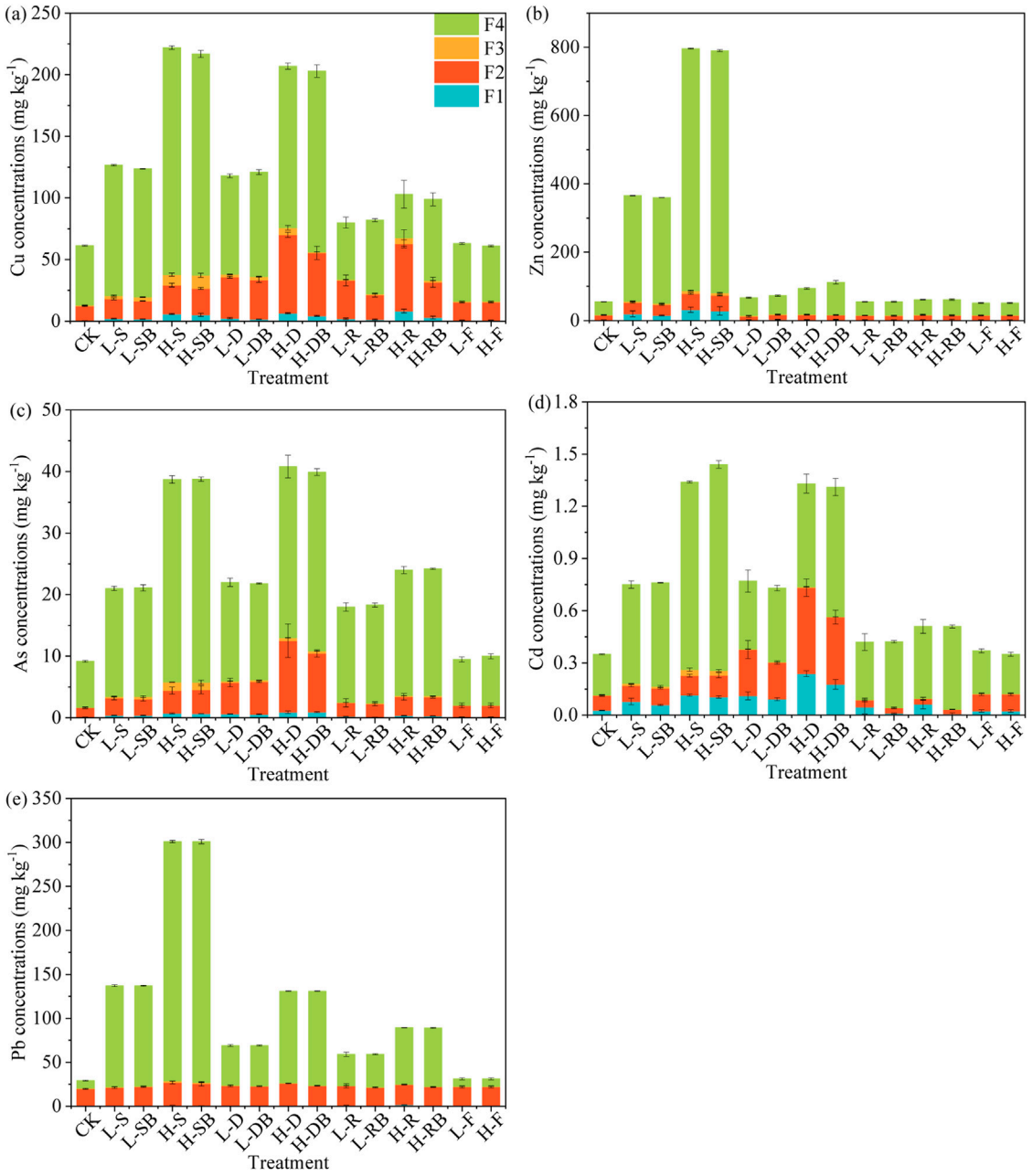

FIGURE 1
Concentrations of Cu **(a)**, Zn **(b)**, As **(c)**, Cd **(d)**, and Pb **(e)** fractions in the soils collected at the rice maturity stage in the greenhouse experiment (mean ± SD, n = 3).

dust, and rainfall addition treatments, respectively. Both results demonstrated that the impact of biochar on the reduction of bioavailable As concentrations is less significant than other cationic HMs (Figure 2).

3.3 HM accumulations in rice plants

The soil applications of slug, dust, and rainwater and foliar applications of dust significantly reduced the biomass of rice tissue ($p < 0.05$), while the biochar improved these (Supplementary Table S4). Significantly higher Cu, Cd, and As concentrations and their BAFs calculated from Equation 2 were observed in rice tissues when dust was added to soils (simulating atmospheric dry deposition) compared to the addition of similar amounts of these HMs using slag (Figure 2; Supplementary Tables S5, S6). According to the Cd mass balance (Equation 1), HMs in rainfall are most readily incorporated into the grains (12%–23% for Cu, 40%–42% for Zn, 1.1. –2.1% for As, 181%–271% for Cd, and 0.58%–0.87% for Pb), followed by HMs in dust, and least from HMs in slag (Table 3). Similar results were also observed in other tissues (root, stem, leaf, and husk, Supplementary Table S7). Additionally, when exposed to

10.3389/fenvs.2025.1734892

TABLE 2 DGT-measured HM concentrations in soils and HM concentrations in soil solutions (mean ± SD, n = 3).

Treatment	pH	DGT-measured concentrations (μg L^{-1})					Soil solution (μg L^{-1})	
		Cu	Zn	As	Cd	Pb	Cu	Cd
CK	6.8 ± 0.085a	0.59 ± 0.13a	52 ± 8.3a	6.5 ± 0.49a	4.5 ± 0.3a	0.17 ± 0.031a	1.56 ± 0.15a	0.11 ± 0.013a
L-S	6.6 ± 0.13b	2.3 ± 0.67c	108 ± 9.1c	18 ± 1.3b	6.8 ± 1.1bd	0.35 ± 0.07b	2.49 ± 0.17b	0.28 ± 0.014b
L-SB	6.9 ± 0.15ac	5.1 ± 0.67c	92 ± 21bc	17 ± 1.2b	6.2 ± 0.69bf	0.22 ± 0.028c	2.15 ± 0.17b	0.21 ± 0.014c
H-S	6.3 ± 0.093d	7.4 ± 0.91e	167 ± 7.9d	27 ± 5.4cd	9.6 ± 1.4ce	0.55 ± 0.064d	3.18 ± 0.33c	0.33 ± 0.028def
H-SB	6.6 ± 0.12b	4.6 ± 0.59d	148 ± 7.6e	25 ± 2.9e	6.1 ± 0.8b	0.47 ± 0.055d	2.54 ± 0.22bd	0.23 ± 0.018c
L-D	6.3 ± 0.25de	5 ± 3.8cde	85 ± 10b	60 ± 2.6f	8.1 ± 0.29c	0.36 ± 0.018b	2.93 ± 0.23d	0.35 ± 0.019d
L-DB	6.7 ± 0.13ab	4.1 ± 1.5d	60 ± 7.3a	61 ± 3.7f	7 ± 0.58d	0.26 ± 0.021c	2.35 ± 0.11b	0.24 ± 0.009c
H-D	6.4 ± 0.08d	21 ± 7.6b	104 ± 14c	92 ± 7.1g	11.3 ± 0.4e	0.47 ± 0.023d	3.82 ± 0.28e	0.38 ± 0.023e
H-DB	6.7 ± 0.18ab	8.9 ± 6.5de	90 ± 9.9b	92 ± 4g	8.1 ± 0.76c	0.38 ± 0.067b	3.17 ± 0.28c	0.29 ± 0.023b
L-R	6.5 ± 0.25db	6.1 ± 1.2ce	109 ± 13c	22 ± 1.5c	6.5 ± 2f	0.38 ± 0.015b	2.98 ± 0.21d	0.28 ± 0.018b
L-RB	6.8 ± 0.13a	3.9 ± 2.4cd	92 ± 5.5b	21 ± 1c	5.4 ± 0.73bf	0.30 ± 0.035bc	2.21 ± 0.19b	0.22 ± 0.016c
H-R	6.3 ± 0.18de	16 ± 6.9b	165 ± 12d	33 ± 2d	7.7 ± 0.65d	0.47 ± 0.041d	3.26 ± 0.28ce	0.34 ± 0.023d
H-RB	6.7 ± 0.12db	12 ± 17abcde	128 ± 11f	32 ± 1.9d	6.3 ± 0.9b	0.35 ± 0.035b	2.7 ± 0.22bd	0.31 ± 0.018f
L-F	6.6 ± 0.11b	0.57 ± 0.11a	50 ± 4.1a	6.8 ± 0.59a	4.4 ± 0.6a	0.19 ± 0.013a	1.46 ± 0.11a	0.11 ± 0.009a
H-F	6.7 ± 0.12a	0.61 ± 0.09a	53 ± 5.3a	6.4 ± 0.43a	4.7 ± 0.7a	0.18 ± 0.022a	1.59 ± 0.21a	0.12 ± 0.018a

1. In the same column, different lowercase letters indicate significant differences among treatments at the $p < 0.05$ level (two-tailed ANOVA followed by Duncan's multiple range test).
2. Zn, As, and Pb concentrations of the soil solution were below the detection limit.

wet deposition, the HM concentrations in the soils were 2.5–13 times lower than slag treatments, but the BAFs for roots and stems were significantly higher than the slag treatments ($p < 0.05$, Supplementary Table S6). Therefore, the BAFs of rice tissues confirmed that HM atmospheric deposition results in particularly high HM bioavailability, which is consistent with the HM fractions in the soils, soil solutions, and DGT extractions. The higher bioavailability and contribution of simulated wet and dry deposition compared to the slag treatments suggest that HM transport in the atmosphere–soil–plant system is not solely determined by content but is also strongly governed by speciation (e.g., F1 of sequential extraction and DGT extraction), which affects uptake and transfer within plant tissues (Table 3; Supplementary Table S7). Additionally, among the metals (except As), Cd had the highest contribution to the rice tissues, while Pb had the lowest. These results suggested that Cd was the most bioavailable HM in rice paddy soils.

We assessed the foliar uptake of HMs by comparing the increased HM amounts in tissues and the applied HM amounts. Foliar uptake contributed up to 16%–32%, 16%–35%, 7.5%–7.6%, 368%–383%, and 0.85%–1.4% of Cu, Zn, As, Cd, and Pb in leaves, respectively, which were higher compared to root exposure to dust (Supplementary Table S7). Increased HM concentrations in other tissues also showed that foliar exposure contributed to 24%–4.2%, 19%–94%, −0.031%–2.0%, 22%–210%, and 0.049%–0.60% of Cu, Zn, As, Cd, and Pb in stems, husks, and grains, respectively. However, As appears to be different from the other HMs and cannot be transported to other tissues, suggesting that atmospheric As cannot accumulate in rice leaves through foliar uptake and that atmospherically deposited As can be taken up via the roots. However, these contributions were much lower than those from root exposure and subsequent transport to these tissues with the same exposure dosages, suggesting less efficient As uptake and translocation rates under direct foliage uptake than root uptake from soils (Table 3).

The HMs in the nodes were also measured to further investigate the differences in transport direction between foliar and root exposures. Root exposure resulted in a bottom-up increase in HM concentrations in the stem nodes (Node Ⅰ ≈ Ⅱ < Ⅲ), which was in contrast to the top-down increase observed during foliage exposures in stem nodes (Node Ⅰ > Ⅱ ≈ Ⅲ) (Supplementary Table S8). When comparing the internal translocation efficiency—defined as the percentage of absorbed HMs transported from the site of uptake (roots or leaves) to other tissues—we found that HMs taken up by leaves were more efficiently translocated to upper tissues (grains and stems) than those taken up by root (Figure 2; Supplementary Table S6). However, the overall uptake efficiency (i.e., the proportion of the externally applied HM dose that successfully enters the plant system) was lower for direct foliar uptake than for root uptake from the soil. This indicates that while a smaller fraction of foliar-deposited HMs entered the plant, a larger proportion of those that did enter were subsequently mobilized to the grains. Additionally, HM concentrations decreased from below- to above-ground tissues (roots > stems > leaves) when HM exposure occurred primarily through soil exposure and subsequent root uptake. This pattern was reversed when the HM source was primarily via foliage exposure (foliage > stems ≈ roots).

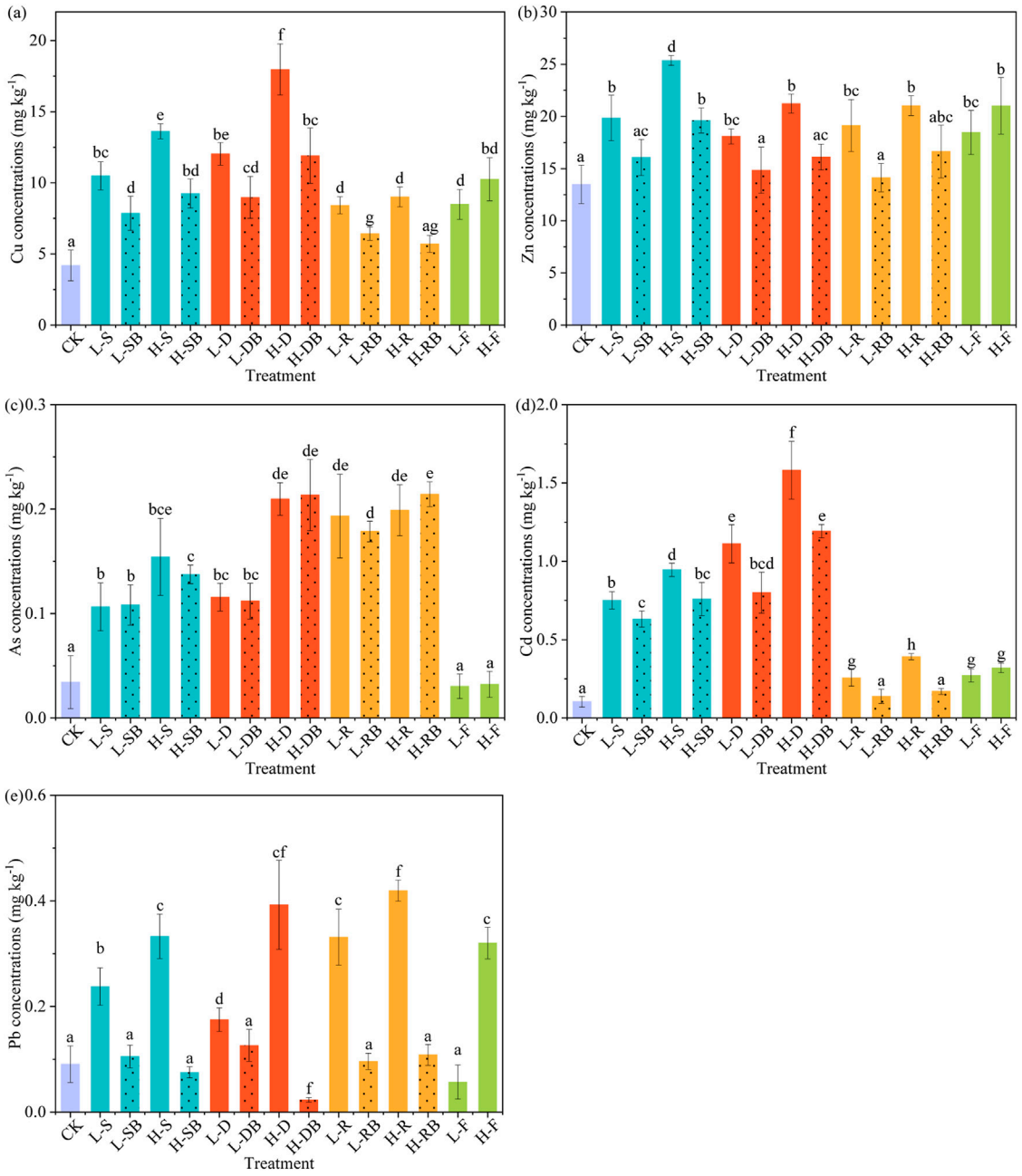

FIGURE 2
Cu **(a)**, Zn **(b)**, As **(c)**, Cd **(d)**, and Pb **(e)** concentrations (dry weight with standard deviations) in rice grain. Data are shown as mean ± SD (n = 3), and different letters show significant difference at $p < 0.05$ level.

The application of soil biochar also significantly reduced HM accumulations in the rice tissues (e.g., F2 and F4). For example, the Cu, Zn, Cd, and Pb concentrations in the grains were significantly reduced by 25%–32%, 19%–23%, 16%–20%, and 54%–73% in the slag treatments, by 25%–34%, 18%–24%, 25%–33%, 25%–28%, and 39%–64% in the dust treatments, and more effectively by 24%–37%, 5%–9%, 32%–45%, 46%–51%, and 70%–74% in the rainfall treatments, respectively, due to the higher mobility of HMs in rainfall. However, the As concentrations were not significantly reduced by any of the biochar treatments, as the bioavailable and soil solution As concentrations were not significantly reduced in these treatments (Figure 1; Table 2).

4 Discussion

High bioavailable HMs fractions in atmospheric dust are consistent with previous studies showing that 13% Cu, 52% Zn, 48% As, 49% Cd, and 10% Pb were presented in the mobile and bioavailable fraction (F1) of dry deposition samples, and more than 90% of HMs were present in dissolved fractions, except for Zn (Xia

TABLE 3 Contribution values (%) of HMs in slag, dust, and rainwater to rice grains in the pot experiment (mean ± SD, n = 3).

Treatment	Contribution (%)				
	Cu	Zn	As	Cd	Pb
L-S	0.36 ± 0.035	0.079 ± 0.0071	0.022 ± 0.0035	6.0 ± 0.42	0.0057 ± 0.00041
L-SB	0.21 ± 0.022	0.032 ± 0.0032	0.023 ± 0.0023	4.9 ± 0.74	0.0014 ± 0.000084
H-S	0.22 ± 0.028	0.059 ± 0.0048	0.015 ± 0.0018	3.1 ± 0.42	0.0035 ± 0.00048
H-SB	0.12 ± 0.011	0.030 ± 0.0030	0.013 ± 0.0012	2.4 ± 0.23	0.00032 ± 0.00021
L-D	0.44 ± 0.061	1.1 ± 0.049	0.025 ± 0.0040	9.8 ± 1.4	0.0081 ± 0.0010
L-DB	0.27 ± 0.064	0.32 ± 0.035	0.024 ± 0.0024	6.8 ± 0.58	0.0029 ± 0.00022
H-D	0.31 ± 0.06	0.74 ± 0.12	0.021 ± 0.0026	5.7 ± 0.46	0.0094 ± 0.0013
H-DB	0.17 ± 0.027	0.25 ± 0.037	0.022 ± 0.0035	4.2 ± 0.43	0.0021 ± 0.00032
L-R	1.0 ± 0.14	0.31 ± 0.026	0.073 ± 0.010	5.4 ± 0.85	0.038 ± 0.0052
L-RB	0.55 ± 0.050	0.055 ± 0.0056	0.066 ± 0.0061	1.3 ± 0.13	0.0044 ± 0.00090
H-R	0.49 ± 0.059	0.47 ± 0.056	0.040 ± 0.0045	5.1 ± 0.62	0.018 ± 0.0021
H-RB	0.15 ± 0.029	0.21 ± 0.034	0.044 ± 0.0085	1.6 ± 0.20	0.0021 ± 0.00043
L-F	0.24 ± 0.075	1.2 ± 0.14	−0.0010±-0.00020	1.6 ± 0.12	0.0022 ± 0.00039
H-F	0.14 ± 0.033	0.72 ± 0.078	0.0010 ± 0.00020	0.81 ± 0.13	0.0015 ± 0.00033

et al., 2024; Xia et al., 2023). These studies also indicate that the atmospheric deposition of HMs is particularly bioavailable and toxic when deposited into terrestrial and aquatic ecosystems (Cui et al., 2024; Fernandez-Olmo et al., 2014). Our results are consistent with these studies, showing high bioavailable fractions and accumulation in rice (Figure 2; Table 3). Among the HMs, the highest bioavailable fractions in soils and contributions to rice tissues are from Cd, which resulted in the most widespread and bioavailable HMs in rice paddy soils, leading to concerns that the rice produced is Cd contaminated (Hou et al., 2020).

To better understand the bioavailability of HMs in soils, the DGT technique has been used as an accurate measure of the labile HM species in soil solutions (Neal-Walthall et al., 2022). DGT results further indicate that HMs from atmospheric deposition are more mobile and bioavailable than those from other sources, such as slag, and are readily accumulated in plants (Table 2). This is because newly deposited trace metals do not form part of the structural components of soil constituents (Shahid et al., 2020). Instead, they tend to preferentially accumulate on the surface of soil aggregates rather than in their core (Wilcke and Kaupenjohann, 1998). These metals on the aggregate surface are more easily mobilized and are more readily available for biological uptake. However, the highly bioavailable HMs from atmospheric deposition were aged in the paddy soils, and the soil aging process closely followed the first-order exponential decay model, with the aging process essentially complete within 60 days (Liu et al., 2022). During this period, approximately 98% of the bioavailable metals changed to unavailable fractions (Zhou et al., 2024b). The rice growth period spanned 90 days, during which nearly all the bioavailable fraction (F1) was converted into other fractions.

The availability of HMs is a critical factor affecting their uptake by crops (Cui et al., 2024). We observed reduced availability of HMs by 4%–91% in F1 fractions, which is attributed to HM interactions with biochar (Figure 1). Biochar surfaces, rich in oxygen-containing functional groups, can form complexes with various HMs, thereby diminishing their bioavailability (Chen et al., 2024). The specific mechanisms of these interactions vary depending on the type of HM. For instance, the formation of Cd and Zn complexes with CO_3^{2-} and PO_4^{2-} is a primary factor in decreasing availability, followed by processes such as cation exchange and chelation (Afzal et al., 2024; Liu H. et al., 2024). In contrast, the main mechanisms affecting Pb and Cu involve cation exchange and coprecipitation (Bogusz and Oleszczuk, 2020). These variations are influenced by the distinct properties of HMs, including their hydrated radius, electronegativity, solubility product constants, and hydrolysis constants (Oral et al., 2024). The biochar applications did not significantly reduce As concentrations in soil bioavailable fractions and rice tissues, which could be attributed to the tendency of As to form negatively charged chemical species such as AsO_4^{3-}, $HAsO_4^{2-}$, and $HAsO_4^{-}$ in alkaline environments (Zhong et al., 2024). Moreover, the hydroxyl groups present on the surface of clay minerals may not have sufficient capacity to bind these negative cations, potentially contributing to the weaker influence of biochar on As bioavailability (Chen et al., 2024).

The utilization of biochar has been shown to have a significantly positive effect on various essential soil properties, such as increasing soil pH, organic carbon content, electrical conductivity (EC), and cation exchange capacity (CEC), indicating a significant improvement of soil characteristics (Chen et al., 2024; Oral et al., 2024). The increase in soil pH levels can be linked to the naturally high pH and ash contents of biochar (Bogusz and Oleszczuk, 2020). Additionally, the release of hydroxides and carbonates by biochar also contributes to the increase in soil pH (Shah et al., 2024). Heightened soil pH leads to an increase in negative charges on

soil particle surfaces, enhancing the binding of HM ions to negatively charged sites, thereby decreasing the availability of soil HM concentrations (Yang et al., 2024). Moreover, the increase in organic carbon and dissolved organic carbon can be attributed to the significant carbon concentrations present in biochar (Li et al., 2024). The surfaces of organic matter in soils contain different functional groups, such as carboxyl and phenolic groups, which can form chemical compounds with HMs (Mandal et al., 2017). Furthermore, the significant elevation in EC and CEC may contribute to a decrease in the bioavailability of HMs in the soil (Roohi et al., 2020). These results suggest that biochar applications can improve soil environmental quality and reduce the exchangeable, soil solution, and DGT-measured HMs in soils, potentially enhancing safe crop production in soils contaminated with HMs. A previous study attributed reduced HM bioaccumulation in rice to decreased HM mobility under biochar applications (Khan et al., 2014). In this study, the main reason for HM reduction in rice is also biochar significantly reducing the bioavailable HMs in soils and soil solutions. This is supported by the significant correlation between HM concentrations in rice tissues and those in F1 fractions, soil solutions, and DGT-measured concentrations ($p < 0.05$). Our results agree with Khan et al. (2020) who reported a 14%–93% decrease in HM bioaccumulation in rice grains due to biochar applications.

Previously, HMs have been considered to be primarily taken up from soils via the root system and subsequently transported to above-ground tissues (Shahid et al., 2017; 2021). Foliar dust applications suggest that rice leaves can directly take up HMs though stomata, aqueous pores, cracks, and lenticels, primarily via the ectodesmata and the subjacent cell symplastic pathway. The observed difference in translocation patterns between foliar and root uptake can be attributed to the distinct pathways of metal transport within the plant. HMs absorbed by roots primarily enter the xylem and are transported upward via the transpiration stream, often resulting in higher accumulation in roots and lower stems (Yamaji and Ma, 2014). In contrast, HMs absorbed through the leaves can enter the phloem, the vascular tissue responsible for distributing photosynthesis (e.g., sugars) from source leaves to sink organs like grains and young stems (Shahid et al., 2017). This phloem mobility facilitates the efficient downward translocation of foliar-absorbed HMs to developing grains, which explains their higher internal translocation efficiency to upper tissues despite a lower overall uptake rate. Regarding foliar uptake, the uptake of particulate-bound HMs is mechanistically different from dissolved ions. These particles can enter leaves through physical pathways such as stomatal openings, aqueous pores, cuticular cracks, or ectodesmata (Yan et al., 2022). Once inside the leaf apoplast, the solubility of the metal species becomes critical. Soluble ions or those released from particles can be taken up by leaf cells via active transport and subsequently load into the phloem for long-distance transport (Shahid et al., 2017; 2021). The lower overall uptake efficiency for foliar application likely reflects the barrier posed by the leaf cuticle and the limited dissolution of particulate metals compared to the direct accessibility of bioavailable HM fractions in the soil solution for roots. Zhou et al. (2024b) calculated the foliar and root uptake of deposited Cd in rice by using a modified isotopic mass balance model and showed that foliar and root uptake of deposited Cd accounted for 47%–51% and 28%–36% in leaves, 41%–45% and 22%–30% in stems, and 45%–49% and 26%–30% in grains, respectively, demonstrating that foliar uptake of HMs may be the dominant method of the rice accumulation.

Previous studies may explain the upward HM transport via the xylem during root exposures and downward HM transport via the phloem during foliar exposures (Shahid et al., 2017). The translocation of HM by the phloem and the distribution of photosynthates from foliage to other tissues occurs though enlarged vascular bundles (EVBs) (Yamaji and Ma, 2014). Hence, active HM transport in rice stimulates both bi-directional xylem and phloem transport (Page and Feller, 2015), and nodes at the location of xylem-to-phloem transfer appear to somewhat limit HM translocation and distribution within plants, as they showed accumulation of HM on one versus the other. Taking Cd as an example, our findings are consistent with the central role of nodes in xylem-to-phloem transfer and plant Cd allocation (Yamaji and Ma, 2019; Zhou et al., 2021), as well as the role of *OsLCT1*—a low-affinity cation transporter in nodes—in Cd loading to the phloem and grain Cd accumulation and re-translocation (Uraguchi et al., 2011; Zhong et al., 2021). This study was conducted as a greenhouse simulation experiment, where atmospheric deposition was administered in a single application. In natural environments, however, deposition occurs dynamically and continuously. Furthermore, changes in the surface functional groups of biochar following aging (e.g., 2–5 years) and the associated risk of heavy metal re-release were not examined. Future research should conduct field *in situ* experiments combined with long-term fixed-position observations to further validate the long-term remediation efficacy of biochar while investigating the migration dynamics of heavy metals under the dynamic input of atmospheric deposition.

It is important to acknowledge the limitations associated with the experimental design employed in this study. Atmospheric deposition in natural ecosystems is a dynamic and continuous process, whereas our simulation involved a single, high-dose application of dust and rainfall to represent several years of deposition. This "shock-loading" approach was necessary to ensure detectable and comparable levels of HM accumulation in rice tissues within a single growth cycle under controlled greenhouse conditions. However, this method may overestimate the instantaneous bioavailability of the newly deposited HMs, as they have not undergone long-term aging processes such as gradual adsorption–desorption equilibrium, diffusion into soil aggregate cores, or lattice fixation, which would typically reduce their bioavailability over time (Liu et al., 2022). The aging process, often following a first-order exponential decay model, can rapidly transform bioavailable fractions into more stable forms within weeks to months (Zhou et al., 2024b). Therefore, while our results conclusively demonstrate the relatively higher bioavailability of HMs from atmospheric deposition compared to slag and the potential of biochar to immobilize them, the absolute contribution rates and immobilization efficiency under continuous, low-level deposition scenarios might be different. Future research should prioritize long-term *in situ* field experiments that incorporate realistic, continuous atmospheric deposition inputs. Such studies, combined with monitoring the aging of biochar itself and the associated long-term stability of immobilized HMs, are crucial for validating the sustained efficacy of biochar as a remediation strategy in dynamically contaminated agricultural systems.

5 Conclusion

This study highlights that atmospherically deposited heavy metal(oid)s (HMs) are more mobile and bioavailable than those in slag. Rice plants preferentially take up atmospherically deposited HMs via both foliar and root pathways, suggesting a high risk of crop contamination in areas with a high load of atmospheric HMs. HMs in rainfall are most readily incorporated into the grains, followed by those in dust, and least from those in slag. The application of biochar was shown to significantly decrease the mobile fractions of HMs in soil, as well as HM concentrations in soil solutions and diffusive gradients in thin films (DGT) extractions, except for As, proving to be an effective method for reducing HM accumulation in rice tissues. Mitigating atmospheric Cd deposition in agricultural environments can lead to a reduction in ecological risks, as atmospheric deposition demonstrates high mobility, availability, and redistribution within plants.

Data availability statement

The original contributions presented in the study are included in the article/Supplementary Material; further inquiries can be directed to the corresponding authors.

Author contributions

ZH: Data curation, Formal Analysis, Conceptualization, Writing – original draft. BD: Writing – review and editing, Investigation, Validation, Resources, Methodology. TS: Formal Analysis, Visualization, Validation, Writing – review and editing, Software, Supervision. DJ: Conceptualization, Writing – review and editing, Funding acquisition, Data curation, Project administration.

Funding

The authors declare financial support was received for the research and/or publication of this article. This study was supported by the National Natural Science Foundation of China (42207277 and U24A20622) and the Jiangxi Provincial Natural Science Foundation (20232ACB213016).

Conflict of interest

The authors declare that the research was conducted in the absence of any commercial or financial relationships that could be construed as a potential conflict of interest.

The handling editor J.Z declared a past co-authorship with the authors B.D and D.J.

Generative AI statement

The authors declare that no Generative AI was used in the creation of this manuscript.

Any alternative text (alt text) provided alongside figures in this article has been generated by Frontiers with the support of artificial intelligence and reasonable efforts have been made to ensure accuracy, including review by the authors wherever possible. If you identify any issues, please contact us.

Publisher's note

Supplementary material

The Supplementary Material for this article can be found online at: https://www.frontiersin.org/articles/10.3389/fenvs.2025.1734892/full#supplementary-material

References

Afzal, S., Alghanem, S. M. S., Alsudays, I. M., Malik, Z., Abbasi, G. H., Ali, A., et al. (2024). Effect of biochar, zeolite and bentonite on physiological and biochemical parameters and lead and zinc uptake by maize (*Zea mays* L.) plants grown in contaminated soil. *J. Hazard. Mater.* 469, 133927. doi:10.1016/j.jhazmat.2024.133927

Bogusz, A., and Oleszczuk, P. (2020). Effect of biochar addition to sewage sludge on cadmium, copper and lead speciation in sewage sludge-amended soil. *Chemosphere* 239, 124719. doi:10.1016/j.chemosphere.2019.124719

Chen, L., Yang, X., Huang, F., Zhu, X., Wang, Z., Sun, S., et al. (2024). Unveiling biochar potential to promote safe crop production in toxic metal (loid) contaminated soil: a meta-analysis. *Environ. Pollut.* 356, 124309. doi:10.1016/j.envpol.2024.124309

Cui, H., Zhao, Y., Hu, K., Xia, R., Zhou, J., and Zhou, J. (2024). Impacts of atmospheric deposition on the heavy metal mobilization and bioavailability in soils amended by lime. *Sci. Total Environ.* 914, 170082. doi:10.1016/j.scitotenv.2024.170082

Ding, S., Jia, F., Xu, D., Sun, Q., Zhang, L., Fan, C., et al. (2011). High-resolution, two-dimensional measurement of dissolved reactive phosphorus in sediments using the diffusive gradients in thin films technique in combination with a routine procedure. *Environ. Sci. and Technol.* 45, 9680–9686. doi:10.1021/es202785p

Du, B., Zhang, H., Ji, D., Huang, Z., Gan, F., and Jun, Z. (2023). *Environmental contamination and health risk assessment to toxic elements in an active lead-zinc mining area. Expos. Health* 15(1), 687–698. doi:10.1007/s12403-022-00515-y

Fang, Z., Li, Y., Li, Y., Yang, D., Zhang, H., Jones, K. C., et al. (2021). Development and applications of novel DGT passive samplers for measuring 12 Per- and polyfluoroalkyl substances in natural waters and wastewaters. *Environ. Science and Technology* 55, 9548–9556. doi:10.1021/acs.est.0c08092

Feng, W., Guo, Z., Xiao, X., Peng, C., Shi, L., Ran, H., et al. (2019). Atmospheric deposition as a source of cadmium and lead to soil-rice system and associated risk assessment. *Ecotoxicol. Environ. Saf.* 180, 160–167. doi:10.1016/j.ecoenv.2019.04.090

Fernandez-Olmo, I., Puente, M., Montecalvo, L., and Irabien, A. (2014). Source contribution to the bulk atmospheric deposition of minor and trace elements in a northern Spanish coastal urban area. *Atmos. Res.* 145, 80–91. doi:10.1016/j.atmosres.2014.04.002

Gao, L., Gao, B., Xu, D., and Liu, L. (2020). DGT: a promising technology for *in-situ* measurement of metal speciation in the environment. *Sci. Total Environ.* 715, 136810. doi:10.1016/j.scitotenv.2020.136810

Hou, D., O'Connor, D., Igalavithana, A. D., Alessi, D. S., Luo, J., Tsang, D. C. W., et al. (2020). Metal contamination and bioremediation of agricultural soils for food safety and sustainability. *Nat. Rev. Earth and Environ.* 1, 366–381. doi:10.1038/s43017-020-0061-y

Islam, M. S., Zhu, J., Xiao, L., Khan, Z. H., Saqib, H. S. A., Gao, M., et al. (2023). Enhancing rice quality and productivity: Multifunctional biochar for arsenic, cadmium, and bacterial control in paddy soil. *Chemosphere* 342, 140157. doi:10.1016/j.chemosphere.2023.140157

Ji, P., Chen, J., Zhou, A., Chen, R., Ding, G., Wang, H., et al. (2023). Anthropogenic atmospheric deposition caused the nutrient and toxic metal enrichment of the enclosed Lakes in north China. *J. Hazardous Materials* 448, 130972. doi:10.1016/j.jhazmat.2023.130972

Khan, A. Z., Khan, S., Khan, M. A., Alam, M., and Ayaz, T. (2020). Biochar reduced the uptake of toxic heavy metals and their associated health risk via rice (*Oryza sativa L.*) grown in Cr-Mn mine contaminated soils. *Environ. Technol. Innov.* 17, 100590. doi:10.1016/j.eti.2019.100590

Khan, S., Reid, B. J., Li, G., and Zhu, Y. G. (2014). Application of biochar to soil reduces cancer risk via rice consumption: a case study in Miaoqian village, Longyan, China. *Environ. Int.* 68, 154–161. doi:10.1016/j.envint.2014.03.017

Li, D., Liu, H., Gao, M., Zhou, J., and Zhou, J. (2022). Effects of soil amendments, foliar sprayings of silicon and selenium and their combinations on the reduction of cadmium accumulation in rice. *Pedosphere* 32, 649–659. doi:10.1016/s1002-0160(21)60052-8

Li, X., Yu, Y., Zhang, Y., Wang, J., and She, D. (2024). Synergistic effects of modified biochar and selenium on reducing heavy metal uptake and improving pakchoi growth in Cd, Pb, Cu, and Zn–contaminated soil. *J. Environ. Chem. Eng.* 12, 113170. doi:10.1016/j.jece.2024.113170

Liu, H.-L., Zhou, J., Li, M., Hu, Y.-M., Liu, X., and Zhou, J. (2019). Study of the bioavailability of heavy metals from atmospheric deposition on the soil-pakchoi (Brassica chinensis L.) system. *J. Hazardous Materials* 362, 9–16. doi:10.1016/j.jhazmat.2018.09.032

Liu, H.-L., Zhou, J., Li, M., Obrist, D., Wang, X.-Z., and Zhou, J. (2021). Chemical speciation of trace metals in atmospheric deposition and impacts on soil geochemistry and vegetable bioaccumulation near a large copper smelter in China. *J. Hazard. Mater.* 413, 125346. doi:10.1016/j.jhazmat.2021.125346

Liu, H., Zhou, J., Li, M., Xia, R., Wang, X., and Zhou, J. (2022). Dynamic behaviors of newly deposited atmospheric heavy metals in the soil-pak choi system. *Environ. Sci. and Technol.* 56, 12734–12744. doi:10.1021/acs.est.2c04062

Liu, H., Chen, C., Li, X., and Yang, P. (2024a). Meta-analysis compares the effectiveness of modified biochar on cadmium availability. *Front. Environ. Sci.* 12, 1413047. doi:10.3389/fenvs.2024.1413047

Liu, Q., Wu, T., Wu, Q., Zhang, C., Wu, D., Zhang, L., et al. (2024b). Effects of soil amendment and foliar selenium applications on cadmium immobilization in soil and accumulation in wheat. *Pedosphere* 34, 1123–1135. doi:10.1016/j.pedsph.2023.07.010

Luo, X., Bing, H., Luo, Z., Wang, Y., and Jin, L. (2019). Impacts of atmospheric particulate matter pollution on environmental biogeochemistry of trace metals in soil-plant system: a review. *Environ. Pollut.* 255, 113138. doi:10.1016/j.envpol.2019.113138

Mandal, S., Sarkar, B., Bolan, N., Ok, Y. S., and Naidu, R. (2017). Enhancement of chromate reduction in soils by surface modified biochar. *J. Environ. Manag.* 186, 277–284. doi:10.1016/j.jenvman.2016.05.034

McLaughlin, M., Smolders, E., Zhao, F., Grant, C., and Montalvo, D. (2021). Managing cadmium in agricultural systems. *Adv. Agron.* 166, 1–129. doi:10.1016/bs.agron.2020.10.004

Mi, Y., Zhou, J., Liu, M., Liang, J., Kou, L., Xia, R., et al. (2023). Machine learning method for predicting cadmium concentrations in rice near an active copper smelter based on chemical mass balance. *Chemosphere* 319, 138028. doi:10.1016/j.chemosphere.2023.138028

Neal-Walthall, N., Ndu, U., Rivera, N. A., Elias, D. A., and Hsu-Kim, H. (2022). Utility of diffusive gradient in thin-film passive samplers for predicting mercury methylation potential and bioaccumulation in freshwater wetlands. *Environ. Sci. and Technol.* 56, 1743–1752. doi:10.1021/acs.est.1c06796

Oral, B., Cosgun, A., Gunay, M. E., and Yildirim, R. (2024). Machine learning-based exploration of biochar for environmental management and remediation. *J. Environmental Management* 360, 121162. doi:10.1016/j.jenvman.2024.121162

Page, V., and Feller, U. (2015). Heavy metals in crop plants: transport and redistribution processes on the whole plant level. *Agronomy* 5, 447–463. doi:10.3390/agronomy5030447

Peng, H., Chen, Y., Weng, L., Ma, J., Ma, Y., Li, Y., et al. (2019). Comparisons of heavy metal input inventory in agricultural soils in north and south China: a review. *Sci. Total Environ.* 660, 776–786. doi:10.1016/j.scitotenv.2019.01.066

Roohi, R., Jafari, M., Jahantab, E., Aman, M. S., Moameri, M., and Zare, S. (2020). Application of artificial neural network model for the identification the effect of municipal waste compost and biochar on phytoremediation of contaminated soils. *J. Geochem. Explor.* 208, 106399. doi:10.1016/j.gexplo.2019.106399

Sachdeva, S., Kumar, R., Sahoo, P. K., and Nadda, A. K. (2023). Recent advances in biochar amendments for immobilization of heavy metals in an agricultural ecosystem: a systematic review. *Environ. Pollut.* 319, 120937. doi:10.1016/j.envpol.2022.120937

Shah, S. S. H., Nakagawa, K., Yokoyama, R., and Berndtsson, R. (2024). Heavy metal immobilization and radish growth improvement using Ca(OH)2-treated cypress biochar in contaminated soil. *Chemosphere* 360, 142385. doi:10.1016/j.chemosphere.2024.142385

Shahid, M., Dumat, C., Khalid, S., Schreck, E., Xiong, T., and Niazi, N. K. (2017). Foliar heavy metal uptake, toxicity and detoxification in plants: a comparison of foliar and root metal uptake. *J. Hazard. Mater.* 325, 36–58. doi:10.1016/j.jhazmat.2016.11.063

Shahid, M., Dumat, C., Niazi, N. K., Xiong, T. T., Farooq, A. B. U., Khalid, S., et al. (2020). Ecotoxicology of heavy metal(loid)-enriched particulate matter: foliar accumulation by plants and health impacts. *Rev. Environmental Contamination Toxicology* 253, 1–49. doi:10.1007/398_2019_38

Shahid, M., Dumat, C., Niazi, N. K., Xiong, T. T., Farooq, A. B. U., and Khalid, S. (2021). "Ecotoxicology of heavy metal (loid)-enriched particulate matter: foliar accumulation by plants and health impacts," in *Reviews of environmental contamination and toxicology*. Editor P. de Voogt (Cham: Springer International Publishing), 65–113.

Shen, X., Huang, D.-Y., Ren, X.-F., Zhu, H.-H., Wang, S., Xu, C., et al. (2016). Phytoavailability of Cd and Pb in crop straw biochar-amended soil is related to the heavy metal content of both biochar and soil. *J. Environ. Manag.* 168, 245–251. doi:10.1016/j.jenvman.2015.12.019

Shoaib, A., and Javaid, A. (2021). "Oxidative stress in plants exposed to heavy metals," in *Organic solutes, oxidative stress, and antioxidant enzymes under abiotic stressors*. London: CRC Press, Taylor & Francis Group, 133–152.

Uraguchi, S., Kamiya, T., Sakamoto, T., Kasai, K., Sato, Y., Nagamura, Y., et al. (2011). Low-affinity cation transporter (OsLCT1) regulates cadmium transport into rice grains. *Proc. National Academy Sciences* 108, 20959–20964. doi:10.1073/pnas.1116531109

Wilcke, W., and Kaupenjohann, M. (1998). Heavy metal distribution between soil aggregate core and surface fractions along gradients of deposition from the atmosphere. *Geoderma* 83, 55–66. doi:10.1016/s0016-7061(97)00134-1

Xia, R., Zhou, J., Sun, Y., Zeng, Z., Liu, H., Cui, H., et al. (2023). Stable isotope ratios trace the rice uptake of cadmium from atmospheric deposition *via* leaves and roots. *Environ. Sci. and Technol.* 57, 16873–16883. doi:10.1021/acs.est.3c04820

Xia, R., Zhou, J., Mi, Y., Cui, H., Liu, H., Hu, K., et al. (2024). Chemical fractions of trace metals in atmospheric wet and dry deposition and contribution to rice root and foliar uptake. *Plant Soil* 494, 285–299. doi:10.1007/s11104-023-06274-2

Xiong, T., Dumat, C., Dappe, V., Vezin, H., Schreck, E., Shahid, M., et al. (2017). Copper oxide nanoparticle foliar uptake, phytotoxicity, and consequences for sustainable urban agriculture. *Environ. Sci. and Technol.* 51, 5242–5251. doi:10.1021/acs.est.6b05546

Yamaji, N., and Ma, J. F. (2014). The node, a hub for mineral nutrient distribution in graminaceous plants. *Trends Plant Sci.* 19, 556–563. doi:10.1016/j.tplants.2014.05.007

Yamaji, N., and Ma, J. F. (2019). Bioimaging of multiple elements by high-resolution LA-ICP-MS reveals altered distribution of mineral elements in the nodes of rice mutants. *Plant J.* 99, 1254–1263. doi:10.1111/tpj.14410

Yan, Z., Yang, M.-Y., Zhao, B.-G., Li, G., Chao, Q., Tian, F., et al. (2022). OsAPL controls the nutrient transport systems in the leaf of rice (Oryza sativa L.). *Planta* 256, 11. doi:10.1007/s00425-022-03913-3

Yang, L., Gao, N., Lv, J., Ling, G., and Zhang, P. (2024). Polysaccharide modified biochar for environmental remediation: types, mechanisms, applications, and engineering significance - a review. *Chem. Eng. J.* 493, 152783. doi:10.1016/j.cej.2024.152783

Zhong, S., Li, X., Li, F., Liu, T., Huang, F., Yin, H., et al. (2021). Water management alters cadmium isotope fractionation between shoots and nodes/leaves in a soil-rice system. *Environ. Sci. and Technol.* 55, 12902–12913. doi:10.1021/acs.est.0c04713

Zhong, R., Pan, D., Huang, G., Yang, G., Wang, X., Niu, R., et al. (2024). Colloidal fraction on pomelo peel-derived biochar plays a dual role as electron shuttle and adsorbent in controlling arsenic transformation in anoxic paddy soil. *Sci. Total Environ.* 934, 173340. doi:10.1016/j.scitotenv.2024.173340

Zhou, C., Gao, Y., Gaulier, C., Luo, M., Zhang, X., Bratkic, A., et al. (2020a). Advances in understanding mobilization processes of trace metals in marine sediments. *Environ. Sci. and Technol.* 54, 15151–15161. doi:10.1021/acs.est.0c05954

Zhou, J., Du, B., Liu, H., Cui, H., Zhang, W., Fan, X., et al. (2020b). The bioavailability and contribution of the newly deposited heavy metals (copper and lead) from atmosphere to rice (Oryza sativa L.). *J. Hazard. Mater.* 384, 121285. doi:10.1016/j.jhazmat.2019.121285

Zhou, J., Gao, M., Cui, H., Li, D., Xia, R., Wang, T., et al. (2021). Influence of silicon and selenium and contribution of the node to cadmium allocation and toxicity in rice. *ACS Agric. Sci. and Technol.* 1, 550–557. doi:10.1021/acsagscitech.1c00157

Zhou, J., Cui, H., Zhu, Z., Liu, M., Xia, R., Liu, X., et al. (2024a). Long-term and multipoint observations of atmospheric heavy metal (cu and cd) deposition and accumulation in soil–crop system and human health risk evaluation around a large smelter. *Expo. Health* 16, 475–487. doi:10.1007/s12403-023-00574-9

Zhou, J., Xia, R., Landis, J. D., Sun, Y., Zeng, Z., and Zhou, J. (2024b). Isotope evidence for rice accumulation of newly deposited and soil legacy cadmium: a three-year field study. *Environ. Sci. and Technol.* 58, 17283–17294. doi:10.1021/acs.est.4c00659

Zhu, C., Tian, H., and Hao, J. (2020). Global anthropogenic atmospheric emission inventory of twelve typical hazardous trace elements, 1995-2012. *Atmos. Environ.* 220, 117061. doi:10.1016/j.atmosenv.2019.117061